Supplementary Materials for

Analyzing density-driven errors: Principles and pitfalls

SEHUN KIM[a], DO-GYEONG LEE[a], GYUMIN KIM[a], YOUNGSAM KIM[a],
MIHIRA SOGAL[b], STEVEN CRISOSTOMO[c], KIERON BURKE[b,c], AND EUNJI SIM[a*]

[a]Department of Chemistry, Yonsei University, 50 Yonsei-ro Seodaemun-gu, Seoul 03722, Korea.

[b]Department of Chemistry, University of California, Irvine, CA 92697, USA

[c]Department of Physics and Astronomy, University of California, Irvine, CA 92697, USA

CONTENTS

*esim@yonsei.ac.kr

SI. TABLES FOR ONE-ELECTRON SYSTEMS

This section contains tables for one-electron systems such as the H atom and various structures of H_2^+. Table S1 contains the geometry information for the one-electron systems used in Sec. IV1 of the main text. Tables S2- S6 demonstrate, in the same format as Table 2 in the main text, that ideal-DDE and pragmatic-DDE are similar for various one-electron systems across eight exchange-correlation functionals, whereas EDI is not.

Table S1: (x, y, z) geometries of H_2^+ at selected bond lengths, taken from the SIE4x4 subset of the GMTKN55 database[1]. All geometries are given in angstroms (Å).

equilibrium			
H	0	0	-0.528637
H	0	0	0.528637
1.25 × equilibrium			
H	0	0	-0.660796
H	0	0	0.660796
1.5 × equilibrium			
H	0	0	-0.792956
H	0	0	0.792956
1.75 × equilibrium			
H	0	0	-0.925115
H	0	0	0.925115

Table S2: Ideal and pragmatic density-driven errors, as well as the energetic density interpolator (in mH), for several functionals evaluated on densities generated with varying mixing parameter a in H_2^+ at equilibrium bond length. In the pragmatic row, the exchange-correlation (XC) functional varies with a as defined in Eq. 17, whereas in the EDI row, the functional is applied directly in Eq. 11 without accounting for this variation. All calculations use the aug-cc-pV5Z basis set[2].

(mH)		Value of a								
Functional	Type	0	0.25	0.5	0.75	1	1.25	1.5	1.75	2
	ideal	0.66	0.36	0.16	0.04	0.00	0.04	0.15	0.33	0.58
SVWN	prag.	-0.63	-0.35	-0.16	-0.04	0.00	-0.04	-0.15	-0.34	-0.59
	EDI	-0.63	-0.59	-0.47	-0.27	0.00	0.34	0.75	1.22	1.75
	ideal	1.25	0.67	0.28	0.07	0.00	0.06	0.24	0.51	0.87
PBE	prag.	-1.14	-0.62	-0.27	-0.07	0.00	-0.06	-0.25	-0.54	-0.95
	EDI	-1.14	-1.06	-0.83	-0.47	0.00	0.56	1.20	1.91	2.68
	ideal	1.62	0.87	0.37	0.09	0.00	0.08	0.30	0.64	1.09
BLYP	prag.	-1.47	-0.80	-0.35	-0.09	0.00	-0.08	-0.31	-0.69	-1.20
	EDI	-1.46	-1.36	-1.06	-0.60	0.00	0.72	1.53	2.42	3.38
	ideal	0.91	0.49	0.21	0.05	0.00	0.05	0.18	0.39	0.67
B3LYP	prag.	-0.84	-0.46	-0.20	-0.05	0.00	-0.05	-0.19	-0.41	-0.72
	EDI	-0.84	-0.78	-0.61	-0.35	0.00	0.42	0.91	1.46	2.06
	ideal	0.62	0.34	0.14	0.04	0.00	0.03	0.13	0.27	0.47
PBE0	prag.	-0.58	-0.32	-0.14	-0.03	0.00	-0.03	-0.13	-0.29	-0.50
	EDI	-0.58	-0.54	-0.42	-0.24	0.00	0.29	0.64	1.02	1.44
	ideal	0.16	0.09	0.04	0.01	0.00	0.01	0.04	0.08	0.13
r^2SCAN50	prag.	-0.15	-0.08	-0.04	-0.01	0.00	-0.01	-0.04	-0.08	-0.14
	EDI	-0.15	-0.14	-0.11	-0.06	0.00	0.08	0.18	0.28	0.41
	ideal	0.67	0.37	0.16	0.04	0.00	0.04	0.14	0.30	0.52
CAM-B3LYP	prag.	-0.63	-0.35	-0.15	-0.04	0.00	-0.04	-0.14	-0.32	-0.56
	EDI	-0.63	-0.59	-0.46	-0.26	0.00	0.32	0.70	1.13	1.61
	ideal	0.62	0.33	0.14	0.03	0.00	0.03	0.12	0.27	0.46
LC-ωPBE	prag.	-0.57	-0.32	-0.14	-0.03	0.00	-0.03	-0.13	-0.28	-0.50
	EDI	-0.57	-0.53	-0.42	-0.24	0.00	0.29	0.63	1.01	1.42

Table S3: Ideal and pragmatic density-driven errors, as well as the energetic density interpolator (in mH), for several functionals evaluated on densities generated with varying mixing parameter a in the H atom. In the pragmatic row, the exchange-correlation (XC) functional varies with a as defined in Eq. 17, whereas in the EDI row, the functional is applied directly in Eq. 11 without accounting for this variation. All calculations use the aug-cc-pV5Z basis set[2].

		Value of a								
Functional	Type	0	0.25	0.5	0.75	1	1.25	1.5	1.75	2
SVWN	ideal	1.02	0.57	0.25	0.06	0.00	0.06	0.24	0.53	0.93
	prag.	-0.99	-0.55	-0.24	-0.06	0.00	-0.06	-0.24	-0.53	-0.94
	EDI	-0.99	-0.92	-0.73	-0.43	0.00	0.54	1.18	1.94	2.80
PBE	ideal	0.65	0.34	0.14	0.03	0.00	0.03	0.11	0.25	0.42
	prag.	-0.57	-0.31	-0.14	-0.03	0.00	-0.03	-0.12	-0.27	-0.46
	EDI	-0.57	-0.53	-0.41	-0.23	0.00	0.27	0.59	0.93	1.29
BLYP	ideal	0.74	0.39	0.16	0.04	0.00	0.04	0.13	0.28	0.48
	prag.	-0.66	-0.36	-0.16	-0.04	0.00	-0.04	-0.14	-0.31	-0.53
	EDI	-0.66	-0.61	-0.47	-0.27	0.00	0.32	0.68	1.07	1.50
r^{2}SCAN	ideal	0.19	0.10	0.04	0.01	0.00	0.01	0.04	0.08	0.13
	prag.	-0.17	-0.10	-0.04	-0.01	0.00	-0.01	-0.04	-0.08	-0.14
	EDI	-0.17	-0.16	-0.13	-0.07	0.00	0.09	0.18	0.29	0.41
B3LYP	ideal	0.40	0.22	0.09	0.02	0.00	0.02	0.08	0.17	0.29
	prag.	-0.37	-0.20	-0.09	-0.02	0.00	-0.02	-0.08	-0.18	-0.31
	EDI	-0.37	-0.34	-0.27	-0.15	0.00	0.18	0.40	0.64	0.90
PBE0	ideal	0.29	0.16	0.07	0.02	0.00	0.02	0.06	0.12	0.21
	prag.	-0.27	-0.15	-0.06	-0.02	0.00	-0.02	-0.06	-0.13	-0.23
	EDI	-0.27	-0.25	-0.19	-0.11	0.00	0.13	0.29	0.46	0.64
r^{2}SCAN50	ideal	0.04	0.02	0.01	0.00	0.00	0.00	0.01	0.02	0.04
	prag.	-0.04	-0.02	-0.01	0.00	0.00	0.00	-0.01	-0.02	-0.04
	EDI	-0.04	-0.04	-0.03	-0.02	0.00	0.02	0.05	0.08	0.11
CAM-B3LYP	ideal	0.47	0.25	0.11	0.03	0.00	0.03	0.10	0.22	0.37
	prag.	-0.44	-0.24	-0.11	-0.03	0.00	-0.03	-0.10	-0.22	-0.39
	EDI	-0.44	-0.41	-0.32	-0.19	0.00	0.23	0.50	0.80	1.14
LC-ωPBE	ideal	0.30	0.16	0.07	0.02	0.00	0.02	0.06	0.14	0.24
	prag.	-0.28	-0.16	-0.07	-0.02	0.00	-0.02	-0.06	-0.14	-0.25
	EDI	-0.28	-0.26	-0.21	-0.12	0.00	0.15	0.32	0.51	0.72

Table S4: Ideal and pragmatic density-driven errors, as well as the energetic density interpolator (in mH), for several functionals evaluated on densities generated with varying mixing parameter a in H_2^+ at 1.25 times the equilibrium bond length. In the pragmatic row, the exchange-correlation (XC) functional varies with a as defined in Eq. 17, whereas in the EDI row, the functional is applied directly in Eq. 11 without accounting for this variation. All calculations use the aug-cc-pV5Z basis set[2].

(mH)		Value of a								
Functional	Type	0	0.25	0.5	0.75	1	1.25	1.5	1.75	2
	ideal	0.95	0.52	0.22	0.06	0.00	0.05	0.20	0.45	0.78
SVWN	prag.	-0.90	-0.50	-0.22	-0.05	0.00	-0.05	-0.21	-0.46	-0.81
	EDI	-0.90	-0.84	-0.66	-0.38	0.00	0.47	1.03	1.66	2.37
	ideal	2.08	1.11	0.47	0.11	0.00	0.10	0.38	0.82	1.38
PBE	prag.	-1.87	-1.03	-0.44	-0.11	0.00	-0.10	-0.40	-0.88	-1.53
	EDI	-1.87	-1.74	-1.36	-0.77	0.00	0.91	1.94	3.08	4.29
	ideal	2.66	1.42	0.60	0.14	0.00	0.13	0.48	1.03	1.74
BLYP	prag.	-2.40	-1.31	-0.57	-0.14	0.00	-0.13	-0.51	-1.12	-1.94
	EDI	-2.40	-2.22	-1.73	-0.98	0.00	1.16	2.47	3.90	5.41
	ideal	1.25	0.67	0.29	0.07	0.00	0.06	0.24	0.51	0.87
r^2SCAN	prag.	-1.14	-0.63	-0.27	-0.07	0.00	-0.06	-0.25	-0.55	-0.95
	EDI	-1.14	-1.06	-0.83	-0.47	0.00	0.57	1.21	1.93	2.70
	ideal	1.51	0.81	0.35	0.08	0.00	0.08	0.29	0.63	1.08
B3LYP	prag.	-1.39	-0.77	-0.33	-0.08	0.00	-0.08	-0.31	-0.67	-1.18
	EDI	-1.39	-1.29	-1.01	-0.58	0.00	0.70	1.49	2.38	3.34
	ideal	1.03	0.56	0.24	0.06	0.00	0.05	0.21	0.44	0.76
PBE0	prag.	-0.96	-0.53	-0.23	-0.06	0.00	-0.05	-0.21	-0.47	-0.82
	EDI	-0.96	-0.89	-0.70	-0.40	0.00	0.48	1.04	1.66	2.34
	ideal	0.29	0.16	0.07	0.02	0.00	0.02	0.06	0.14	0.24
r^2SCAN50	prag.	-0.27	-0.15	-0.07	-0.02	0.00	-0.02	-0.06	-0.14	-0.25
	EDI	-0.27	-0.25	-0.20	-0.12	0.00	0.14	0.31	0.51	0.73
	ideal	1.01	0.55	0.24	0.06	0.00	0.05	0.21	0.45	0.77
CAM-B3LYP	prag.	-0.94	-0.52	-0.23	-0.06	0.00	-0.05	-0.21	-0.47	-0.82
	EDI	-0.94	-0.88	-0.69	-0.40	0.00	0.48	1.04	1.67	2.36
	ideal	0.90	0.48	0.21	0.05	0.00	0.05	0.17	0.38	0.64
LC-ωPBE	prag.	-0.82	-0.45	-0.20	-0.05	0.00	-0.05	-0.18	-0.40	-0.70
	EDI	-0.82	-0.76	-0.60	-0.34	0.00	0.41	0.88	1.41	1.98

Table S5: Ideal and pragmatic density-driven errors, as well as the energetic density interpolator (in mH), for several functionals evaluated on densities generated with varying mixing parameter a in H_2^+ at 1.5 times the equilibrium bond length. In the pragmatic row, the exchange-correlation (XC) functional varies with a as defined in Eq. 17, whereas in the EDI row, the functional is applied directly in Eq. 11 without accounting for this variation. All calculations use the aug-cc-pV5Z basis set[2].

(mH)		Value of a								
Functional	Type	0	0.25	0.5	0.75	1	1.25	1.5	1.75	2
	ideal	1.36	0.75	0.32	0.08	0.00	0.07	0.29	0.63	1.08
SVWN	prag.	-1.29	-0.71	-0.31	-0.08	0.00	-0.08	-0.30	-0.65	-1.15
	EDI	-1.29	-1.20	-0.95	-0.54	0.00	0.67	1.45	2.33	3.31
	ideal	3.12	1.66	0.70	0.17	0.00	0.15	0.57	1.21	2.04
PBE	prag.	-2.81	-1.54	-0.67	-0.16	0.00	-0.15	-0.60	-1.31	-2.27
	EDI	-2.81	-2.60	-2.03	-1.15	0.00	1.36	2.90	4.57	6.35
	ideal	3.88	2.08	0.88	0.21	0.00	0.19	0.71	1.51	2.55
BLYP	prag.	-3.52	-1.93	-0.83	-0.20	0.00	-0.19	-0.75	-1.64	-2.85
	EDI	-3.52	-3.26	-2.55	-1.44	0.00	1.71	3.63	5.73	7.95
	ideal	2.00	1.07	0.45	0.11	0.00	0.10	0.38	0.81	1.37
r^2SCAN	prag.	-1.82	-1.00	-0.43	-0.11	0.00	-0.10	-0.39	-0.87	-1.51
	EDI	-1.82	-1.69	-1.32	-0.75	0.00	0.90	1.92	3.04	4.25
	ideal	2.22	1.20	0.51	0.12	0.00	0.11	0.44	0.94	1.60
B3LYP	prag.	-2.05	-1.13	-0.49	-0.12	0.00	-0.12	-0.45	-1.00	-1.74
	EDI	-2.05	-1.91	-1.50	-0.85	0.00	1.03	2.21	3.52	4.94
	ideal	1.57	0.85	0.36	0.09	0.00	0.08	0.31	0.67	1.14
PBE0	prag.	-1.45	-0.80	-0.35	-0.09	0.00	-0.08	-0.32	-0.71	-1.23
	EDI	-1.45	-1.35	-1.06	-0.60	0.00	0.73	1.56	2.50	3.51
	ideal	0.45	0.25	0.11	0.03	0.00	0.03	0.10	0.22	0.38
r^2SCAN50	prag.	-0.43	-0.24	-0.11	-0.03	0.00	-0.03	-0.10	-0.22	-0.39
	EDI	-0.43	-0.40	-0.32	-0.18	0.00	0.23	0.50	0.80	1.15
	ideal	1.40	0.76	0.33	0.08	0.00	0.07	0.29	0.62	1.06
CAM-B3LYP	prag.	-1.31	-0.72	-0.32	-0.08	0.00	-0.08	-0.30	-0.65	-1.14
	EDI	-1.31	-1.22	-0.96	-0.55	0.00	0.67	1.44	2.31	3.27
	ideal	1.20	0.64	0.27	0.07	0.00	0.06	0.23	0.49	0.84
LC-ωPBE	prag.	-1.09	-0.60	-0.26	-0.06	0.00	-0.06	-0.24	-0.52	-0.91
	EDI	-1.09	-1.02	-0.79	-0.45	0.00	0.54	1.16	1.85	2.59

Table S6: Ideal and pragmatic density-driven errors, as well as the energetic interpolator (in mH), for several functionals evaluated on densities generated with varying mixing parameter a in H_2^+ at 1.75 times the equilibrium bond length. In the pragmatic row, the exchange-correlation (XC) functional varies with a as defined in Eq. 17, whereas in the EDI row, the functional is applied directly in Eq. 11 without accounting for this variation. All calculations use the aug-cc-pV5Z basis set[2].

(mH)		Value of a								
Functional	Type	0	0.25	0.5	0.75	1	1.25	1.5	1.75	2
	ideal	1.85	1.01	0.44	0.11	0.00	0.10	0.39	0.85	1.47
SVWN	prag.	-1.75	-0.97	-0.43	-0.11	0.00	-0.10	-0.40	-0.89	-1.56
	EDI	-1.75	-1.63	-1.29	-0.74	0.00	0.91	1.97	3.17	4.49
	ideal	4.22	2.27	0.96	0.23	0.00	0.21	0.78	1.67	2.82
PBE	prag.	-3.85	-2.11	-0.92	-0.22	0.00	-0.21	-0.83	-1.81	-3.14
	EDI	-3.85	-3.57	-2.79	-1.58	0.00	1.88	4.00	6.31	8.77
	ideal	5.08	2.75	1.17	0.28	0.00	0.25	0.97	2.06	3.48
BLYP	prag.	-4.68	-2.58	-1.12	-0.27	0.00	-0.26	-1.02	-2.23	-3.87
	EDI	-4.68	-4.35	-3.41	-1.93	0.00	2.31	4.93	7.79	10.82
	ideal	2.85	1.54	0.65	0.16	0.00	0.14	0.54	1.16	1.97
r^2SCAN	prag.	-2.61	-1.44	-0.62	-0.15	0.00	-0.15	-0.57	-1.25	-2.17
	EDI	-2.61	-2.43	-1.90	-1.08	0.00	1.29	2.76	4.37	6.10
	ideal	2.96	1.61	0.69	0.17	0.00	0.15	0.59	1.28	2.19
B3LYP	prag.	-2.76	-1.53	-0.67	-0.16	0.00	-0.16	-0.62	-1.36	-2.38
	EDI	-2.76	-2.57	-2.02	-1.15	0.00	1.40	3.02	4.81	6.76
	ideal	2.16	1.17	0.50	0.12	0.00	0.11	0.43	0.93	1.58
PBE0	prag.	-2.01	-1.11	-0.48	-0.12	0.00	-0.11	-0.45	-0.98	-1.71
	EDI	-2.01	-1.87	-1.47	-0.83	0.00	1.01	2.17	3.47	4.87
	ideal	0.65	0.36	0.16	0.04	0.00	0.04	0.14	0.31	0.54
r^2SCAN50	prag.	-0.62	-0.35	-0.15	-0.04	0.00	-0.04	-0.15	-0.32	-0.57
	EDI	-0.62	-0.58	-0.46	-0.27	0.00	0.33	0.72	1.16	1.65
	ideal	1.77	0.97	0.42	0.10	0.00	0.10	0.37	0.80	1.38
CAM-B3LYP	prag.	-1.67	-0.93	-0.41	-0.10	0.00	-0.10	-0.38	-0.84	-1.47
	EDI	-1.67	-1.56	-1.23	-0.70	0.00	0.86	1.86	2.99	4.22
	ideal	1.49	0.80	0.34	0.08	0.00	0.07	0.28	0.61	1.03
LC-ωPBE	prag.	-1.36	-0.75	-0.32	-0.08	0.00	-0.08	-0.29	-0.65	-1.13
	EDI	-1.36	-1.26	-0.99	-0.56	0.00	0.67	1.43	2.28	3.19

SII. TABLES FOR MULTI-ELECTRON SYSTEMS

This section contains the tables for multi-electron systems appearing in Sec. V of the main text. Table S7 shows that when analyzing the magnitude of DDEs using proxy benchmark densities for the BH76 dataset, the results frequently do not agree between different proxy benchmark densities. Table S8 shows that for several atoms and their anions, the difference in energy between the CCSD and CCSD(T) densities evaluated using various functionals after Kohn-Sham inversion is very small. Table S9 summarizes the subset, systems, and stoichiometry information for the 103 data points used in Fig. 16 and Fig. 18 in the main text.

Table S7: Proxy-DDEs (in kcal/mol) on the BH76 database of four functionals using LC-ωPBE and SX0.5 proxy benchmark densities. In roughly 1/3 of cases, the proxies disagree on which functional has the lowest DDE. Proxy-DDEs results from Ref.[3].

	LC-ωPBE				SX0.5				
Index	PBE	SCAN	B3LYP	BLYP	PBE	SCAN	B3LYP	BLYP	Disagree?
1	-0.84	-0.43	-0.57	-1.09	-1.73	-0.72	-1.13	-1.95	no
2	-2.32	-1.43	-0.99	-2.57	-3.90	-2.40	-2.01	-4.27	no
3	-0.35	-0.26	-0.28	-0.45	-0.49	-0.46	-0.34	-0.56	**yes**
4	-0.35	-0.26	-0.28	-0.45	-0.49	-0.46	-0.34	-0.56	**yes**
5	-0.95	-0.40	-0.53	-1.16	-1.57	-0.54	-1.05	-1.81	no
6	-0.95	-0.40	-0.53	-1.16	-1.57	-0.54	-1.05	-1.81	no
7	-0.82	-0.57	-0.57	-1.06	-1.20	-0.74	-0.94	-1.57	no
8	-1.05	-0.69	-0.57	-1.10	-1.72	-1.19	-0.77	-1.61	no
9	-1.75	-0.40	-0.46	-1.87	-10.35	-4.02	-5.32	-10.31	no
10	-1.99	-0.71	-0.65	-2.15	-11.19	-5.19	-5.43	-10.91	no
11	-1.99	-0.93	-1.18	-2.31	-3.95	-1.97	-2.41	-4.25	no
12	-2.38	-1.34	-1.34	-2.72	-4.35	-2.47	-2.55	-4.62	no
13	-1.36	-0.89	-0.26	-1.00	-2.29	-1.68	-0.46	-1.57	no
14	-1.36	-0.89	-0.26	-1.00	-2.29	-1.68	-0.46	-1.57	no
15	-0.71	-0.46	-0.10	-0.53	-1.72	-1.32	-0.46	-1.32	no
16	-0.71	-0.46	-0.10	-0.53	-1.72	-1.32	-0.46	-1.32	no
17	-2.14	-1.31	-0.63	-1.82	-1.97	-1.34	-0.47	-1.58	no
18	-2.14	-1.31	-0.63	-1.82	-1.97	-1.34	-0.47	-1.58	no
19	-1.46	-0.86	-0.42	-1.30	-1.49	-1.06	-0.42	-1.27	no
20	-1.46	-0.86	-0.42	-1.30	-1.49	-1.06	-0.42	-1.27	no
21	-1.94	-1.06	-0.52	-1.59	-2.09	-1.36	-0.37	-1.41	no
22	-1.99	-1.11	-0.35	-1.58	-3.16	-1.90	-0.94	-2.73	no
23	-0.55	-0.21	-0.14	-0.44	-0.89	-0.63	-0.22	-0.61	no

Index	LC-ωPBE				SX0.5				Proxies Disagree?
	PBE	SCAN	B3LYP	BLYP	PBE	SCAN	B3LYP	BLYP	
24	-1.71	-0.89	-0.29	-1.45	-2.96	-1.76	-0.97	-2.70	no
25	-1.38	-0.86	-0.28	-1.08	-2.25	-1.54	-0.56	-1.76	no
26	-1.74	-1.13	-0.47	-1.44	-2.13	-1.65	-0.40	-1.49	no
27	-0.87	-0.58	-0.15	-0.68	-1.77	-1.32	-0.53	-1.49	no
28	-1.29	-0.81	-0.31	-1.07	-1.93	-1.39	-0.48	-1.51	no
29	-0.85	-0.39	-0.41	-1.07	-2.56	-0.74	-1.59	-2.82	**yes**
30	-0.07	0.19	-0.05	-0.14	-0.75	-0.17	-0.56	-0.83	**yes**
31	-0.87	-0.56	-0.48	-1.19	-0.96	-0.49	-0.59	-1.29	**yes**
32	-0.40	-0.18	-0.13	-0.48	-0.11	-0.26	0.13	-0.08	no
33	-1.08	-0.97	-0.83	-1.66	-2.03	-0.49	-1.58	-2.59	**yes**
34	-0.82	-0.70	-0.65	-1.18	-1.88	-0.50	-1.20	-2.03	**yes**
35	-2.33	-0.96	-1.10	-2.58	-3.56	-1.08	-2.17	-3.98	no
36	-1.75	-0.54	-0.80	-1.84	-3.11	-0.93	-1.83	-3.26	**yes**
37	-0.03	0.12	0.05	-0.08	-0.51	-0.14	-0.14	-0.41	no
38	0.06	0.13	0.00	-0.05	-0.40	-0.19	-0.15	-0.38	**yes**
39	-0.75	-0.28	-0.27	-0.75	-1.37	-0.43	-0.75	-1.37	no
40	-0.96	-0.48	-0.45	-0.98	-1.30	-0.58	-0.60	-1.23	**yes**
41	-0.99	-0.31	-0.33	-1.03	-2.67	-1.19	-1.14	-2.56	**yes**
42	-0.81	-0.14	-0.23	-0.86	-2.62	-1.04	-1.15	-2.47	**yes**
43	-0.88	-0.40	-0.42	-0.89	-1.62	-0.71	-0.89	-1.64	no
44	-1.09	-0.55	-0.52	-1.17	-2.17	-1.07	-1.10	-2.24	no
45	-0.64	-0.21	-0.13	-0.55	-1.39	-0.53	-0.43	-1.25	**yes**
46	-0.85	-0.38	-0.25	-0.75	-2.11	-0.84	-0.89	-1.98	**yes**
47	-0.87	-0.61	-0.56	-0.98	-1.62	-0.88	-1.01	-1.79	no
48	-0.94	-0.67	-0.64	-1.06	-1.86	-1.11	-1.12	-2.03	no
49	-0.77	-0.60	-0.64	-0.97	-1.31	-0.78	-1.12	-1.54	no
50	-1.20	-1.07	-1.12	-1.50	-2.29	-1.23	-1.81	-2.59	no
51	-0.54	-0.32	-0.32	-0.74	-1.08	-0.47	-0.70	-1.16	no
52	-0.71	-0.59	-0.67	-1.00	-1.52	-0.77	-1.12	-1.81	no
53	-1.00	-0.78	-0.92	-1.37	-1.91	-1.02	-1.47	-2.40	no
54	-1.23	-0.93	-1.09	-1.66	-2.37	-1.16	-1.72	-2.84	no
55	-0.61	-0.43	-0.51	-0.83	-1.11	-0.58	-0.93	-1.40	no
56	-0.81	-0.65	-0.78	-1.10	-1.47	-0.74	-1.27	-1.92	no
57	-0.49	-0.36	-0.41	-0.65	-1.00	-0.49	-0.72	-1.12	no
58	-1.09	-0.76	-0.93	-1.37	-2.04	-0.92	-1.45	-2.37	no
59	-0.90	-0.67	-0.72	-1.12	-1.73	-0.84	-1.17	-2.01	no

Index	LC-ωPBE				SX0.5				Proxies Disagree?
	PBE	SCAN	B3LYP	BLYP	PBE	SCAN	B3LYP	BLYP	
60	-0.77	-0.60	-0.64	-1.01	-1.42	-0.71	-1.08	-1.83	no
61	-1.30	-0.98	-1.17	-1.66	-2.52	-1.24	-1.78	-2.93	no
62	-1.01	-0.72	-0.84	-1.27	-1.90	-0.93	-1.35	-2.31	no
63	-0.73	-0.56	-0.63	-0.97	-1.47	-0.67	-1.04	-1.69	no
64	-1.13	-0.82	-0.99	-1.44	-2.12	-1.01	-1.56	-2.49	no
65	-0.91	-0.66	-0.77	-1.14	-1.70	-0.80	-1.19	-1.96	no
66	-0.88	-0.65	-0.75	-1.08	-1.61	-0.77	-1.14	-1.85	no
67	-0.99	-0.71	-0.85	-1.28	-1.91	-0.89	-1.32	-2.27	no
68	-0.89	-0.63	-0.74	-1.09	-1.66	-0.75	-1.15	-1.98	no
69	-1.11	-0.86	-0.97	-1.37	-2.10	-0.98	-1.44	-2.32	no
70	-0.79	-0.55	-0.66	-1.00	-1.55	-0.66	-1.05	-1.71	no
71	-1.06	-0.81	-0.93	-1.34	-2.01	-0.91	-1.40	-2.19	no
72	-0.98	-0.69	-0.84	-1.26	-1.85	-0.87	-1.30	-2.14	no
73	-0.86	-0.64	-0.71	-1.08	-1.59	-0.72	-1.11	-1.87	no
74	-1.16	-0.88	-1.00	-1.44	-2.28	-1.08	-1.62	-2.61	no
75	-1.06	-0.75	-0.89	-1.32	-2.04	-0.93	-1.42	-2.30	no
76	-0.84	-0.62	-0.69	-1.04	-1.52	-0.71	-1.08	-1.75	no

Table S8: Comparison of total energy differences (in kcal/mol) for several functionals evaluated on CCSD and CCSD(T) densities obtained via Kohn–Sham (KS) inversion for simple atomic systems. In this work, we follow the PySCF implementation: the (T) contribution is included perturbatively to the one–particle density matrix generated from a converged CCSD wavefunction, yielding a perturbatively corrected CCSD density rather than a formally variational (T)–relaxed density.[4–8]

(kcal/mol)	System													
Functional	C	C^-	O	O^-	F	F^-	Si	Si^-	P	P^-	S	S^-	Cl	Cl^-
SVWN	0.04	0.29	0.10	0.50	0.09	0.35	0.04	0.12	0.03	0.25	0.10	0.28	0.11	0.23
PBE	0.01	0.27	0.08	0.50	0.09	0.44	0.03	0.09	0.02	0.16	0.04	0.19	0.06	0.18
BLYP	0.01	0.33	0.10	0.58	0.11	0.49	0.04	0.15	0.05	0.27	0.09	0.30	0.11	0.28
r^2SCAN	-0.06	0.09	-0.01	0.12	0.01	0.20	0.02	0.06	0.02	0.01	-0.04	0.01	-0.04	0.04
B3LYP	-0.02	0.17	0.05	0.22	0.06	0.24	0.03	0.10	0.04	0.14	0.05	0.16	0.06	0.15
PBE0	-0.02	0.08	0.02	0.07	0.03	0.14	0.02	0.04	0.01	0.02	-0.01	0.03	0.00	0.04
r^2SCAN50	-0.08	-0.14	-0.06	-0.44	-0.05	-0.20	0.00	0.01	0.01	-0.12	-0.07	-0.14	-0.08	-0.09
CAM-B3LYP	-0.02	0.08	0.06	0.12	0.07	0.20	0.02	0.06	0.04	0.06	0.05	0.10	0.06	0.12
LC-ωPBE	-0.03	-0.11	0.04	-0.07	0.06	0.12	-0.02	-0.07	-0.01	-0.21	-0.04	-0.15	-0.02	-0.07

Table S9: Subset, systems, and stoichiometry information for the 103 benchmark reactions. Reactions were selected from the GMTKN55[1] dataset based on criteria that ensure CCSD densities can be generated, excluding cases where only hydrogen atoms participate in the reaction. Additionally, the ratio of density-sensitive to density-insensitive reactions was chosen to be approximately balanced for the PBE functional. Four halogen-containing interaction systems were added from the B30 (Bauzá30) dataset [9, 10]. Reaction indices marked with an asterisk (*) correspond to reactions involving only closed-shell or non-degenerate open-shell species, in order to avoid the orbital occupancy variability discussed in Fig. 16.

Reaction Index	Subset	System			Stoichiometry		
1	BH76	RKT10	H2	f	1	-1	-1
2	BH76	RKT01	H2	cl	1	-1	-1
3	BH76	RKT02	oh	H2	1	-1	-1
4*	BH76	fch3fts	fch3fcomp		1	-1	
5	BH76	RKT17	O	hcl	1	-1	-1
6	BH76	RKT17	oh	cl	1	-1	-1
7*	B30	3	2	1	1	-1	-1
8*	B30	6	5	4	1	-1	-1
9*	B30	9	8	7	1	-1	-1
10*	B30	12	11	10	1	-1	-1
11*	WATER27	H2O2	H2O		1	-2	
12*	WATER27	H2O3	H2O		1	-3	
13*	WCPT18	ts1	reac1		1	-1	
14*	WCPT18	ts2	reac2		1	-1	
15*	WCPT18	ts1h2o	reac1	h2o	1	-1	-1
16*	WCPT18	ts2h2o	reac2	h2o	1	-1	-1
17	G21EA	EA_c	EA_c-		1	-1	
18	G21EA	EA_o	EA_o-		1	-1	
19	G21EA	EA_f	EA_f-		1	-1	
20	G21EA	EA_si	EA_si-		1	-1	
21	G21EA	EA_p	EA_p-		1	-1	
22	G21EA	EA_s	EA_s-		1	-1	
23	G21EA	EA_cl	EA_cl-		1	-1	
24	G21EA	EA_8n	EA_8		1	-1	
25*	G21EA	EA_9n	EA_9		1	-1	
26*	G21EA	EA_10n	EA_10		1	-1	
27*	G21EA	EA_12n	EA_12		1	-1	
28	G21EA	EA_13n	EA_13		1	-1	

Table S9

Reaction Index	Subset	Systems			Stoichiometry		
29	G21EA	EA_14n	EA_14		1	-1	
30*	G21EA	EA_15n	EA_15		1	-1	
31*	G21EA	EA_16n	EA_16		1	-1	
32	G21EA	EA_17n	EA_17		1	-1	
33*	G21EA	EA_18n	EA_18		1	-1	
34	G21EA	EA_19n	EA_19		1	-1	
35	G21EA	EA_20n	EA_20		1	-1	
36	G21EA	EA_21n	EA_21		1	-1	
37	G21EA	EA_23n	EA_23		1	-1	
38	G21EA	EA_24n	EA_24		1	-1	
39*	G21EA	EA_25n	EA_25		1	-1	
40*	AHB21	1	1A	1B	1	-1	-1
41*	AHB21	2	2A	2B	1	-1	-1
42*	AHB21	3	3A	3B	1	-1	-1
43*	AHB21	4	4A	4B	1	-1	-1
44*	AHB21	5	5A	5B	1	-1	-1
45*	AHB21	9	9A	9B	1	-1	-1
46	G21IP	b+	b		1	-1	
47	G21IP	c+	c		1	-1	
48	G21IP	n+	n		1	-1	
49	G21IP	o+	o		1	-1	
50	G21IP	f+	f		1	-1	
51	G21IP	al+	al		1	-1	
52	G21IP	si+	si		1	-1	
53	G21IP	p+	p		1	-1	
54	G21IP	s+	s		1	-1	
55	G21IP	cl+	cl		1	-1	
56*	G21IP	IP_59	8		1	-1	
57*	G21IP	IP_60	11		1	-1	
58	G21IP	IP_61	12		1	-1	
59*	G21IP	IP_62	13		1	-1	
60	G21IP	IP_63	14		1	-1	
61*	G21IP	IP_64	18		1	-1	
62	G21IP	IP_65	IP_n65		1	-1	
63*	G21IP	IP_66	19		1	-1	
64*	G21IP	IP_67	20		1	-1	

Table S9

Reaction Index	Subset	Systems					Stoichiometry				
65	G21IP	IP_68	137				1	-1			
66	G21IP	IP_70	22				1	-1			
67	G21IP	IP_71	25				1	-1			
68*	G21IP	IP_72	26				1	-1			
69*	G21IP	IP_74	34				1	-1			
70	G21IP	IP_75	37				1	-1			
71	G21IP	IP_76	43				1	-1			
72	G21IP	IP_77	44				1	-1			
73	G21IP	IP_78	45				1	-1			
74	G21IP	IP_79	51				1	-1			
75*	G2RC	104	40	1			1	-1	-1		
76*	G2RC	18	52	1			2	-1	-1		
77*	G2RC	26	25	1			1	-1	-1		
78	W4-11	h	h2				2	-1			
79	W4-11	c	h	ch4			1	4	-1		
80	W4-11	c	o	h	methanol		1	1	4	-1	
81	W4-11	o	h	h2o			1	2	-1		
82	W4-11	o	h	oh			1	1	-1		
83	W4-11	c	n	h	hcn		1	1	1	-1	
84	W4-11	c	n	h	hnc		1	1	1	-1	
85	W4-11	c	o	h	hco		1	1	1	-1	
86	W4-11	c	o	co			1	1	-1		
87	W4-11	c	o	h	oxirene		2	1	2	-1	
88	W4-11	c	o	f	f2co		1	1	2	-1	
89	W4-11	c	o	n	h	hocn	1	1	1	1	-1
90	W4-11	h	o	hooh			2	2	-1		
91	W4-11	c	o	co2			1	2	-1		
92	W4-11	h	o	cl	hocl		1	1	1	-1	
93	W4-11	n	o	no			1	1	-1		
94	W4-11	cl	cl2				2	-1			
95	W4-11	o	f	of			1	1	-1		
96	W4-11	o	o3				3	-1			
97	W4-11	f	o	f2o			2	1	-1		
98	W4-11	o	o2				2	-1			
99	W4-11	f	f2				2	-1			
100*	W4-11	n	n2				2	-1			

Table S9

Reaction Index	Subset	Systems				Stoichiometry			
101	W4-11	c	f	h	hccf	2	1	1	-1
102	W4-11	h	n	o	c-hono	1	1	2	-1
103	W4-11	h	n	o	t-hono	1	1	2	-1

SIII. FIGURES FOR ONE-ELECTRON SYSTEMS

This section contains figures for one-electron systems. Figures S1- S5 are presented in the same format as Figure 1 in the main text, plotting curves for various exchange-correlation functionals against the exact curve for one-electron systems. The relative positions of the functional curves compared to the exact curve vary depending on the functional.

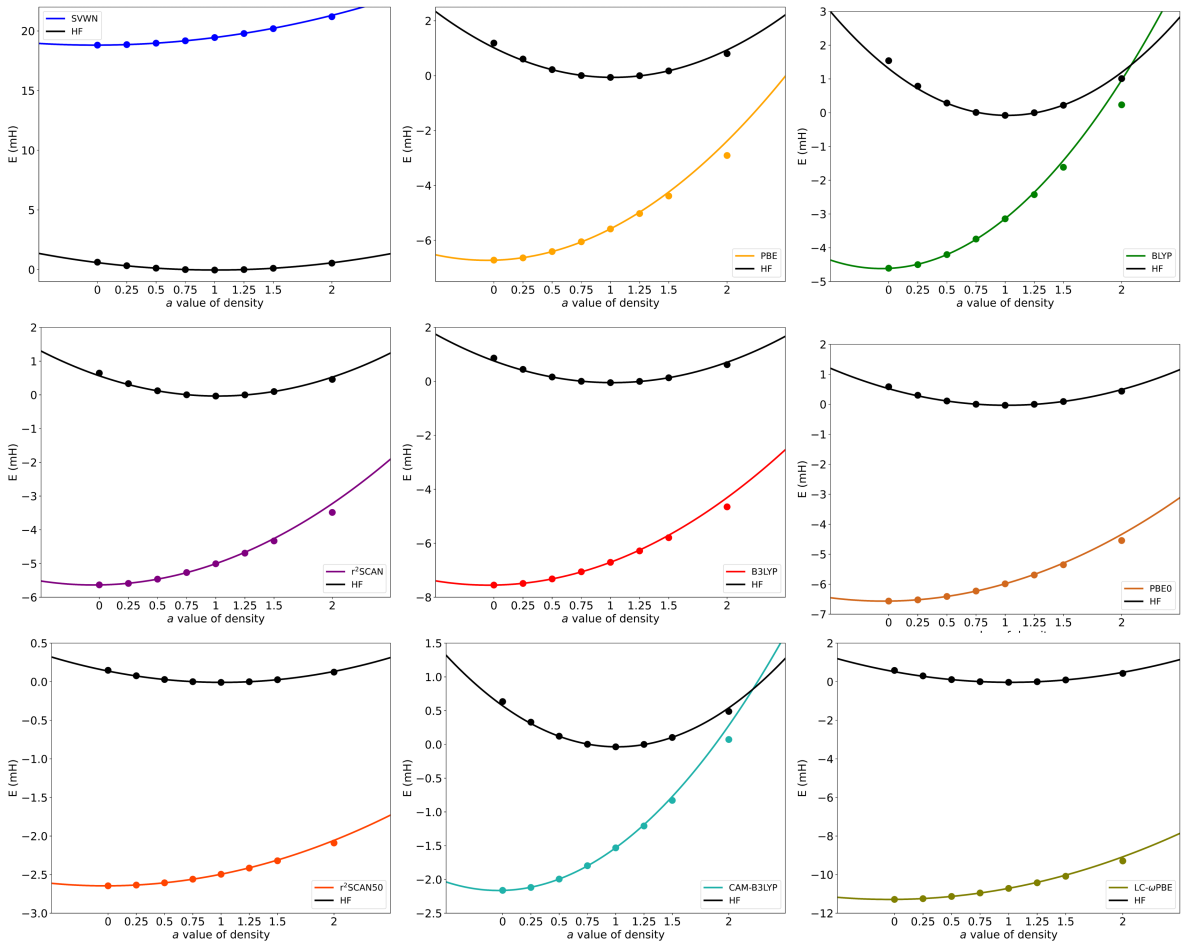

Figure S1: Energy curves of H_2^+ at the equilibrium structure for several functionals (colored) and the exact functional (black), evaluated on the family of densities that minimize the interpolation functional defined in Eq. 17.

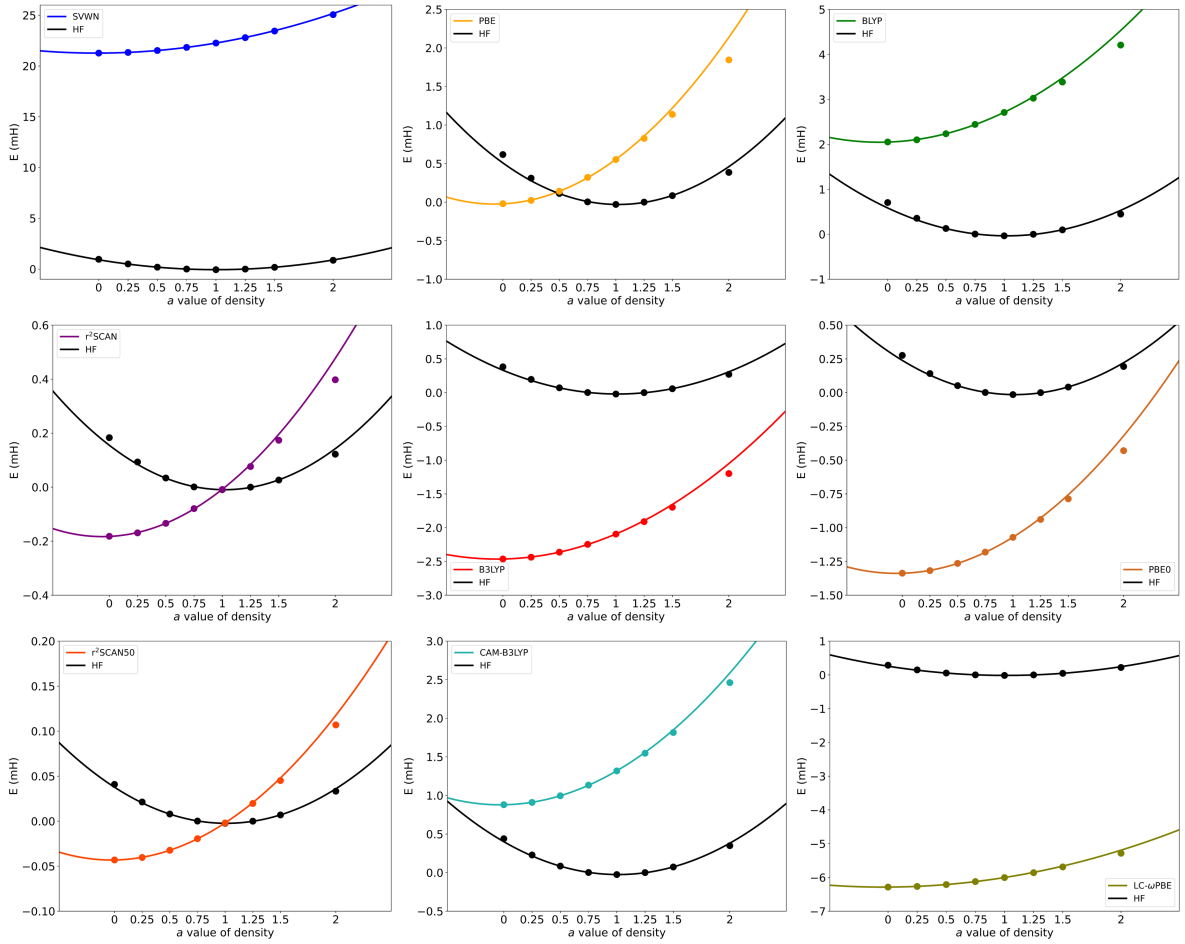

Figure S2: Energy curves of H atom for several functionals (colored) and the exact functional (black), evaluated on the family of densities that minimize the interpolation functional defined in Eq. 17.

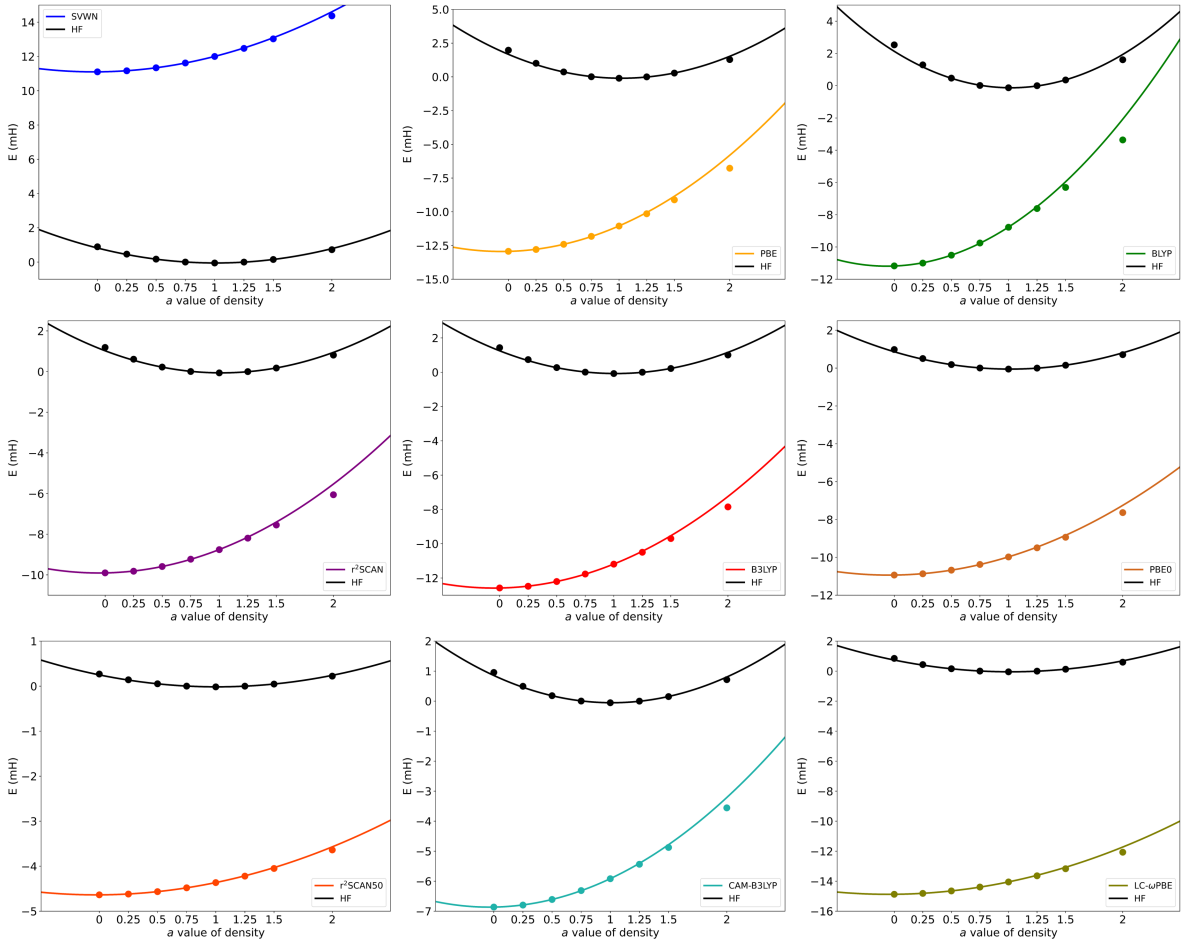

Figure S3: Energy curves of H_2^+ at 1.25 times the equilibrium bond length for several functionals (colored) and the exact functional (black), evaluated on the family of densities that minimize the interpolation functional defined in Eq. 17.

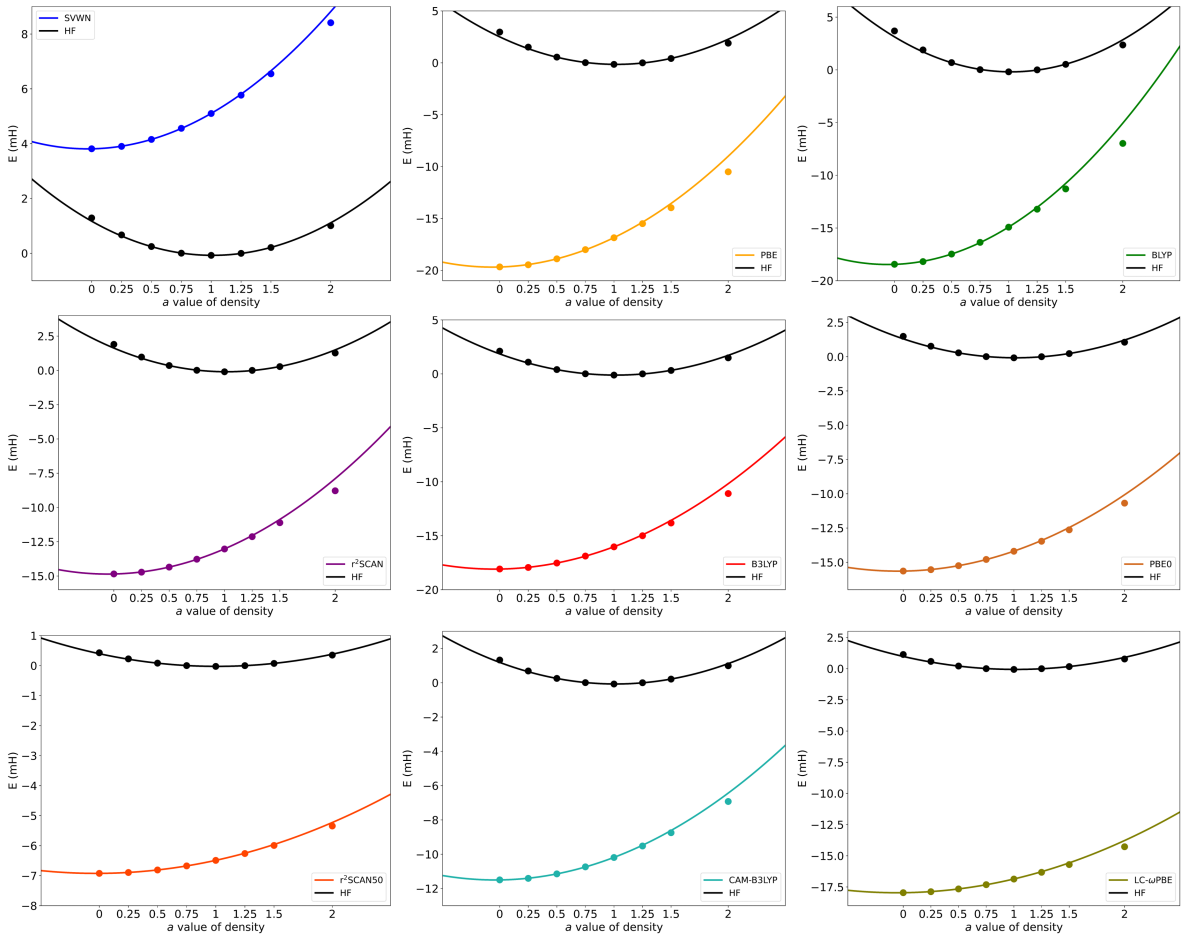

Figure S4: Energy curves of H_2^+ at 1.5 times the equilibrium bond length for several functionals (colored) and the exact functional (black), evaluated on the family of densities that minimize the interpolation functional defined in Eq. 17.

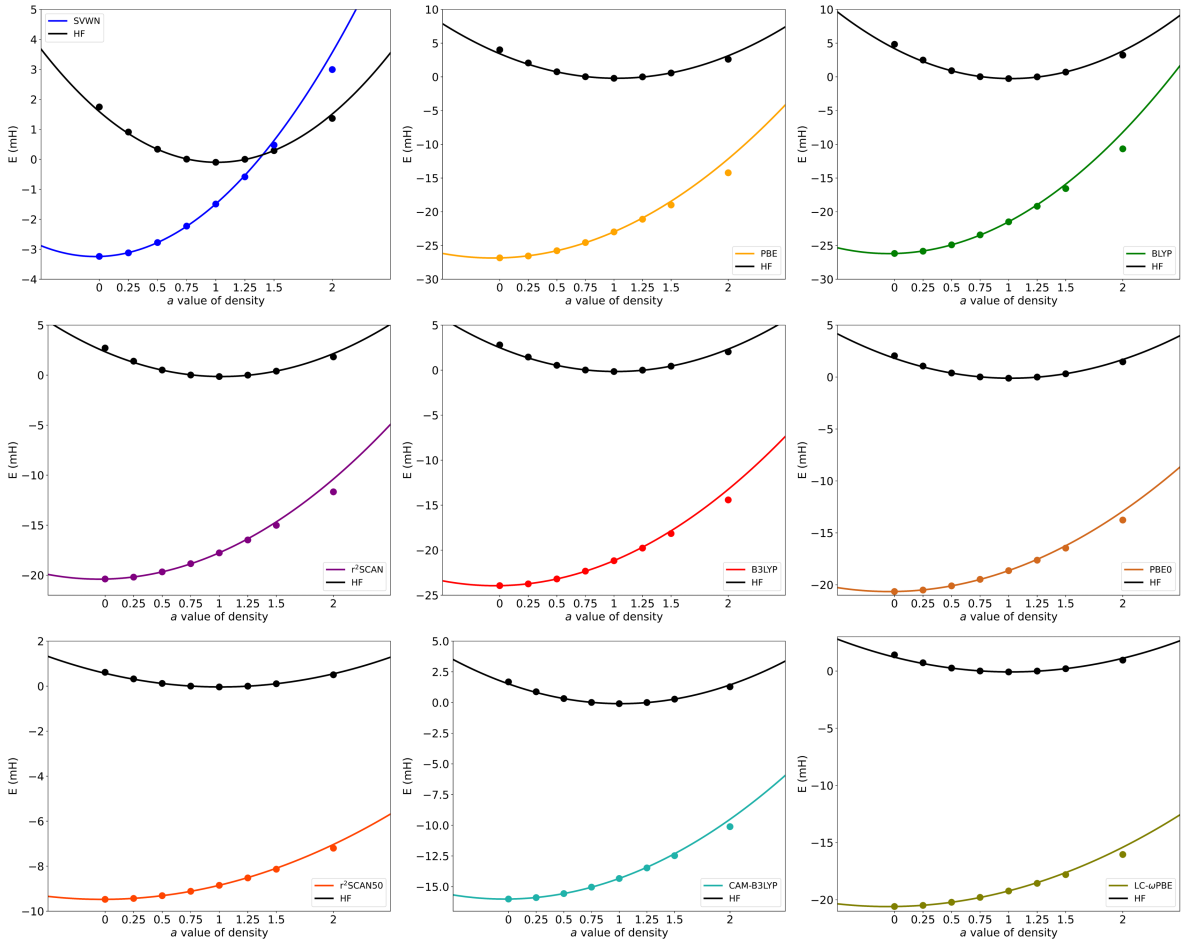

Figure S5: Energy curves of H_2^+ at 1.75 times the equilibrium bond length for several functionals (colored) and the exact functional (black), evaluated on the family of densities that minimize the interpolation functional defined in Eq. 17.

SIV. FIGURES FOR MULTI-ELECTRON SYSTEMS

This section contains the figures for multi-electron systems found in Sec. V of the main text. Figures S6-S7 shows a contour map of the difference between the CCSD and CCSD(T) densities[6–8, 11] for the H···H···F and H···H···Cl transition states, revealing that the difference between the two is very small. Figure S8 shows the distribution of errors between self-consistent DFT and HF-DFT across various functionalities for the 103 reactions in the main text, categorized by density sensitivity. This reveals that in the density-insensitive case, there is little difference in performance between DFT and HF-DFT, but in the density-sensitive case, HF-DFT significantly reduces the error. Figures S9- S18, presented in the same format as Figure 18 in the main text, analyzed the correlation between pragmatic-DDE and four density metrics across various functional models for 103 reactions. However, no significant relationship was found. This demonstrates that differences in density metrics do not directly correlate with DDE.

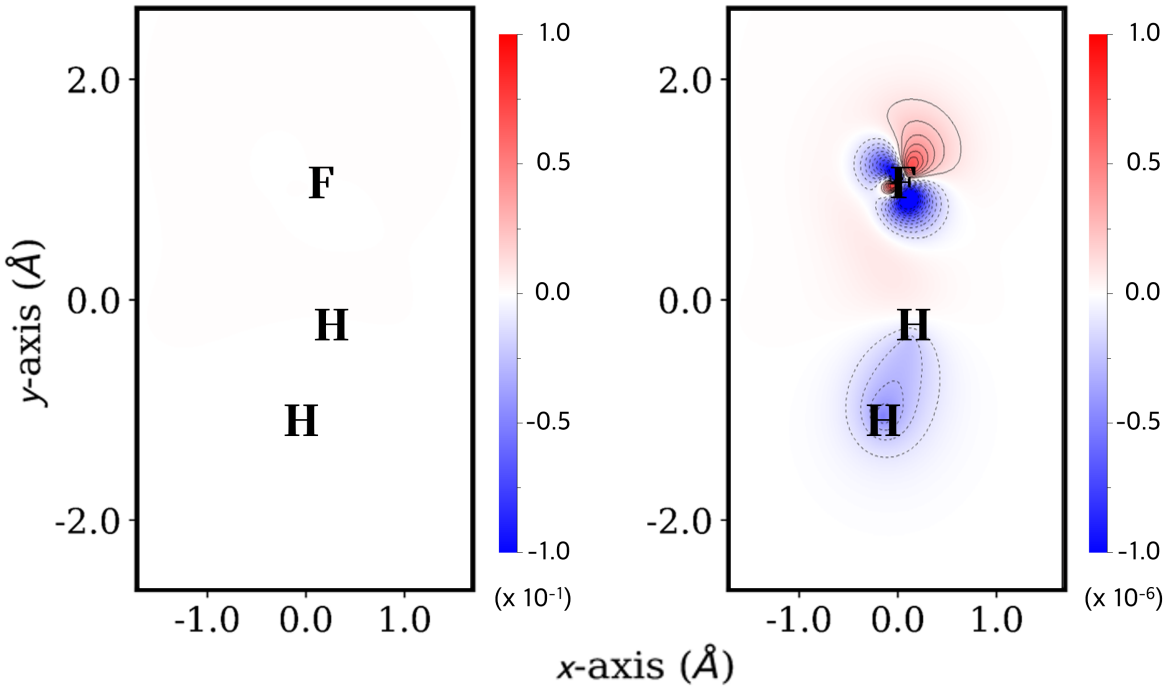

Figure S6: Contour maps of the density error, $n^{CCSD}(\mathbf{r}) - n^{CCSD(T)}(\mathbf{r})$, for the H···H···F transition state. The color scale is the same as in Fig. 14 (left) and scaled down by a factor of 10^{-5} (right). Density units are given in $e/\text{Å}^3$.

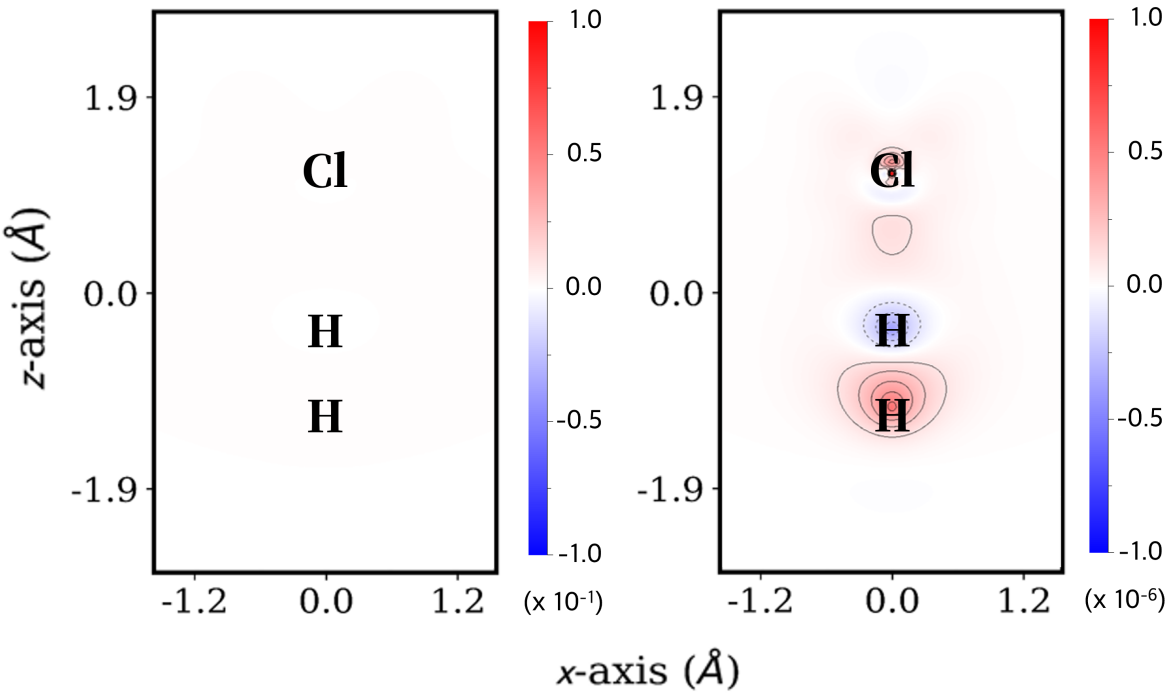

Figure S7: Contour maps of the density error, $n^{CCSD}(\mathbf{r}) - n^{CCSD(T)}(\mathbf{r})$, for the H $\cdots$ H $\cdots$ cl transition state. The color scale is the same as in Fig. 15 (left) and scaled down by a factor of 10^{-5} (right). Density units are given in $e/\text{Å}^3$.

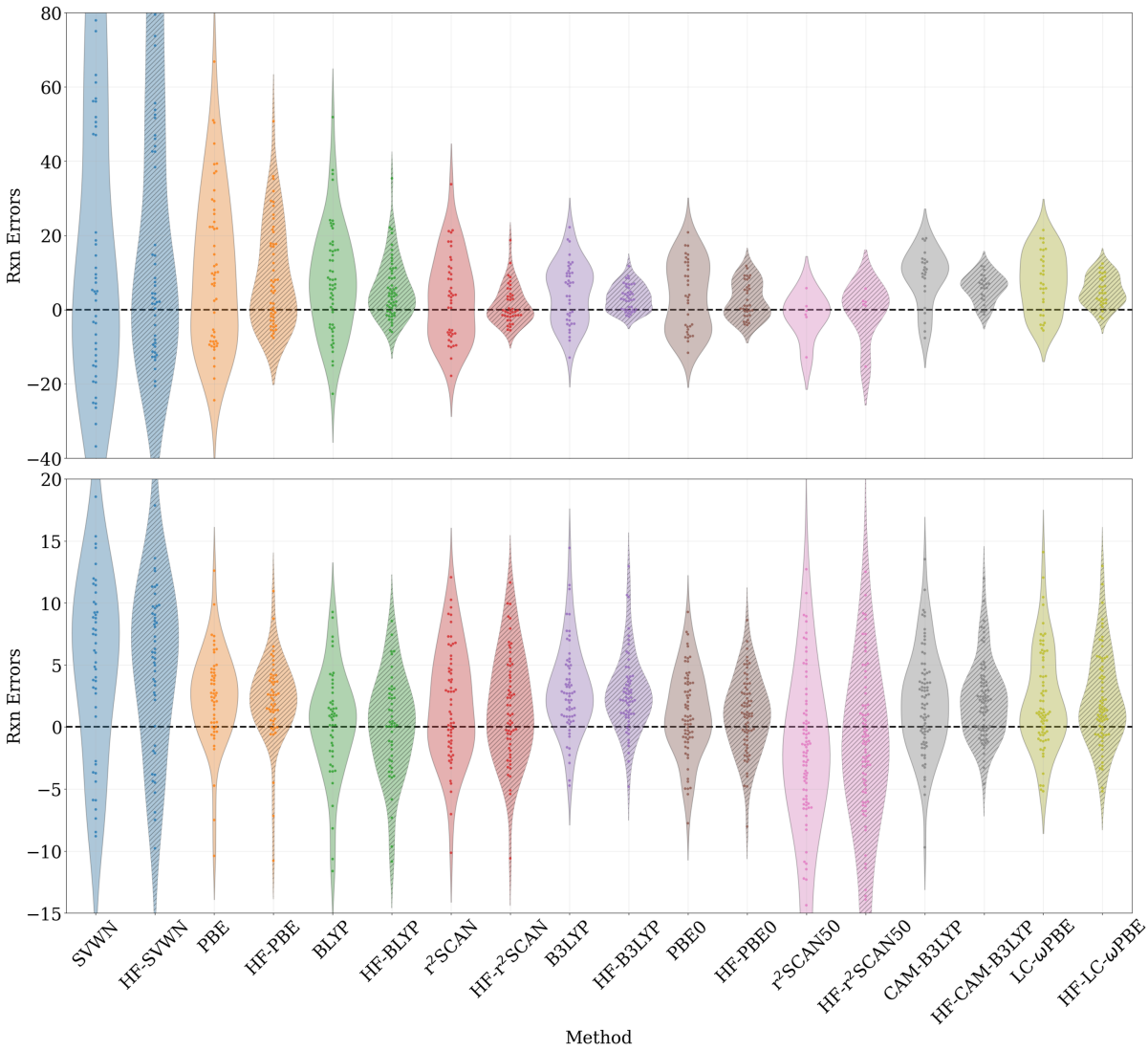

Figure S8: Distributions of reaction energy errors (in kcal/mol) for the 103 benchmark reactions (see Table S9 for the full list): (Top) density-sensitive cases and (Bottom) density-insensitive cases. Reference energies are CCSD(T)/aug-cc-pV5Z.

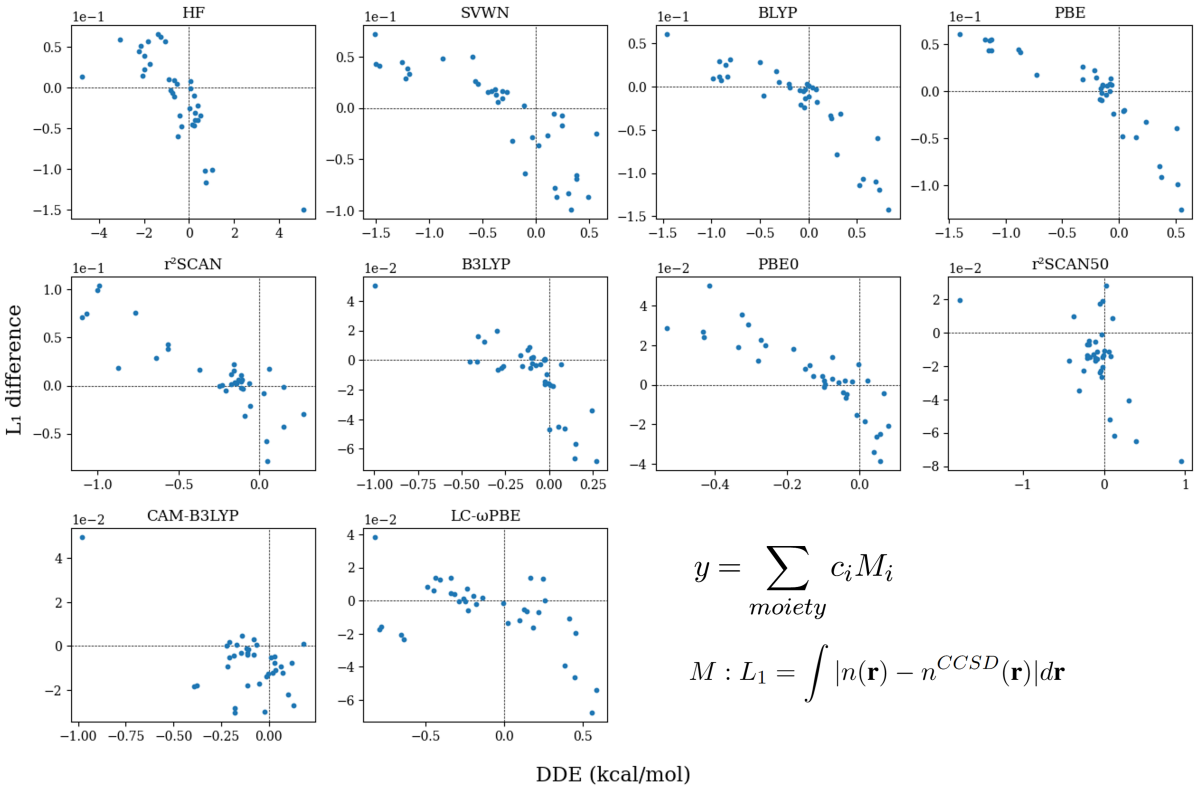

Figure S9: Relation between density-driven error (DDE) and L_1 norm differences for the 36 selected reactions (listed in Table S9), evaluated across various density functionals. CCSD densities are used as the reference. The equation used to calculate the density metric is provided at the bottom right corner of the figure.

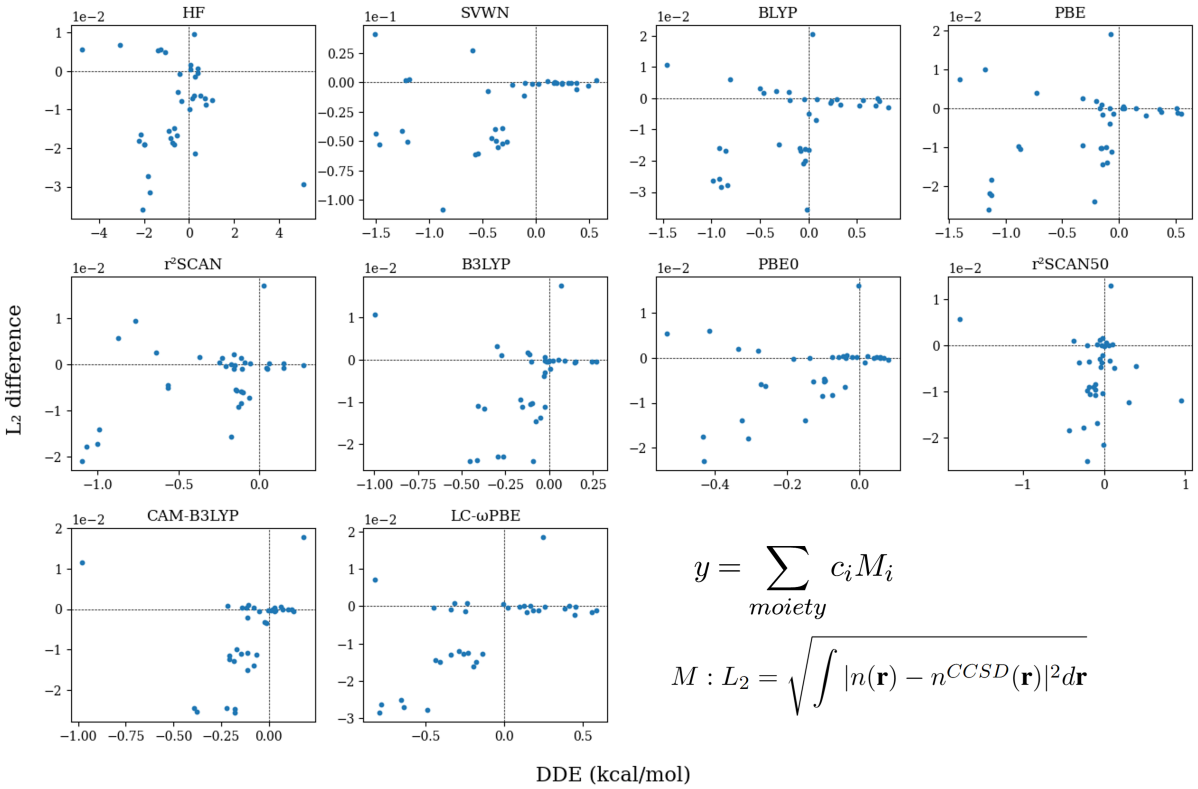

Figure S10: Relation between density-driven error (DDE) and L_2 norm differences for the 36 selected reactions (listed in Table S9), evaluated across various density functionals. CCSD densities are used as the reference. The equation used to calculate the density metric is provided at the bottom right corner of the figure.

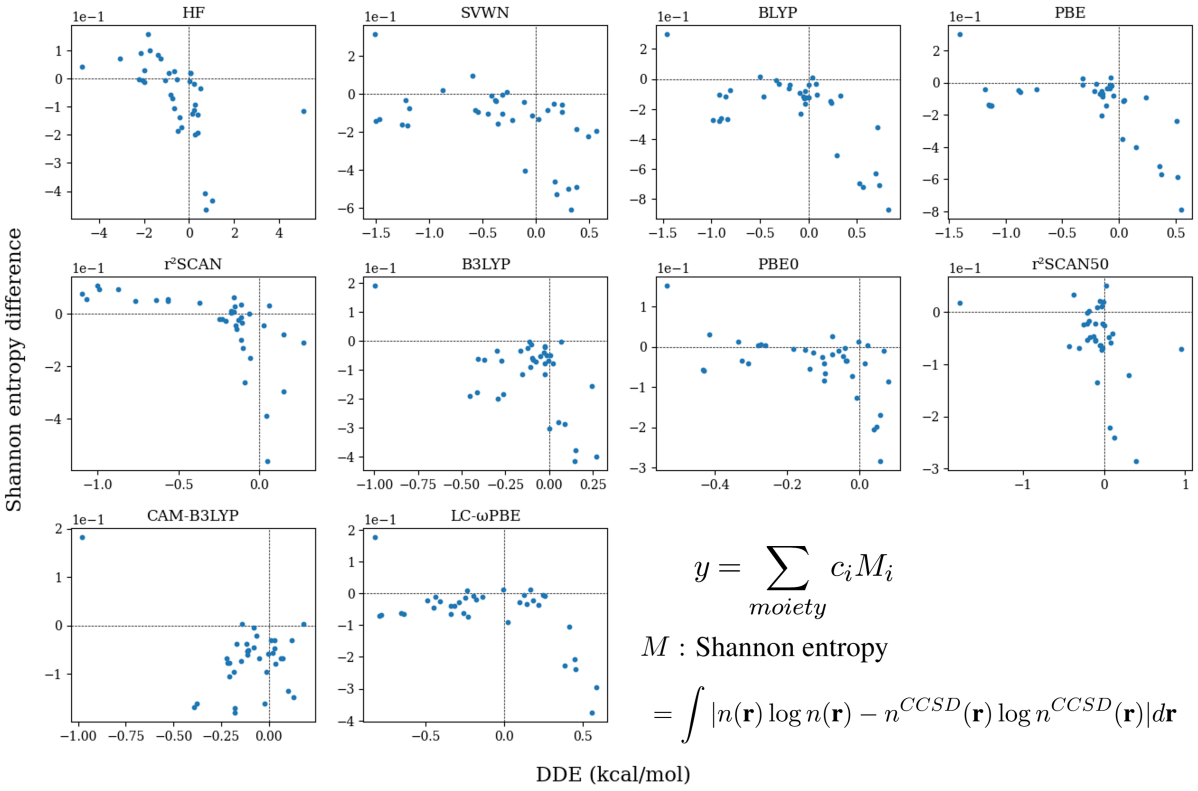

Figure S11: Relation between density-driven error (DDE) and Shannon entropy [12] differences for the 36 selected reactions (listed in Table S9), evaluated across various density functionals. CCSD densities are used as the reference. The equation used to calculate the density metric is provided at the bottom right corner of the figure.

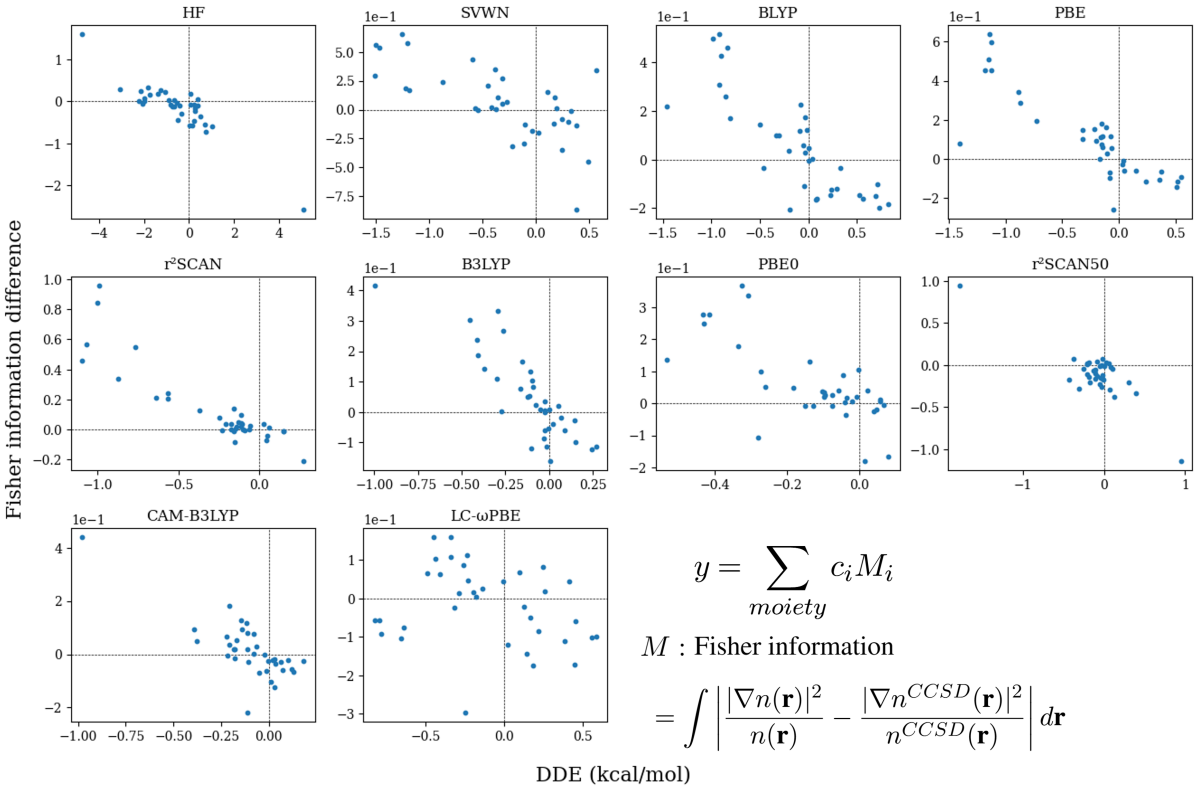

Figure S12: Relation between density-driven error (DDE) and Fisher information [13] differences for the 36 selected reactions (listed in Table S9), evaluated across various density functionals. CCSD densities are used as the reference. The equation used to calculate the density metric is provided at the bottom right corner of the figure.

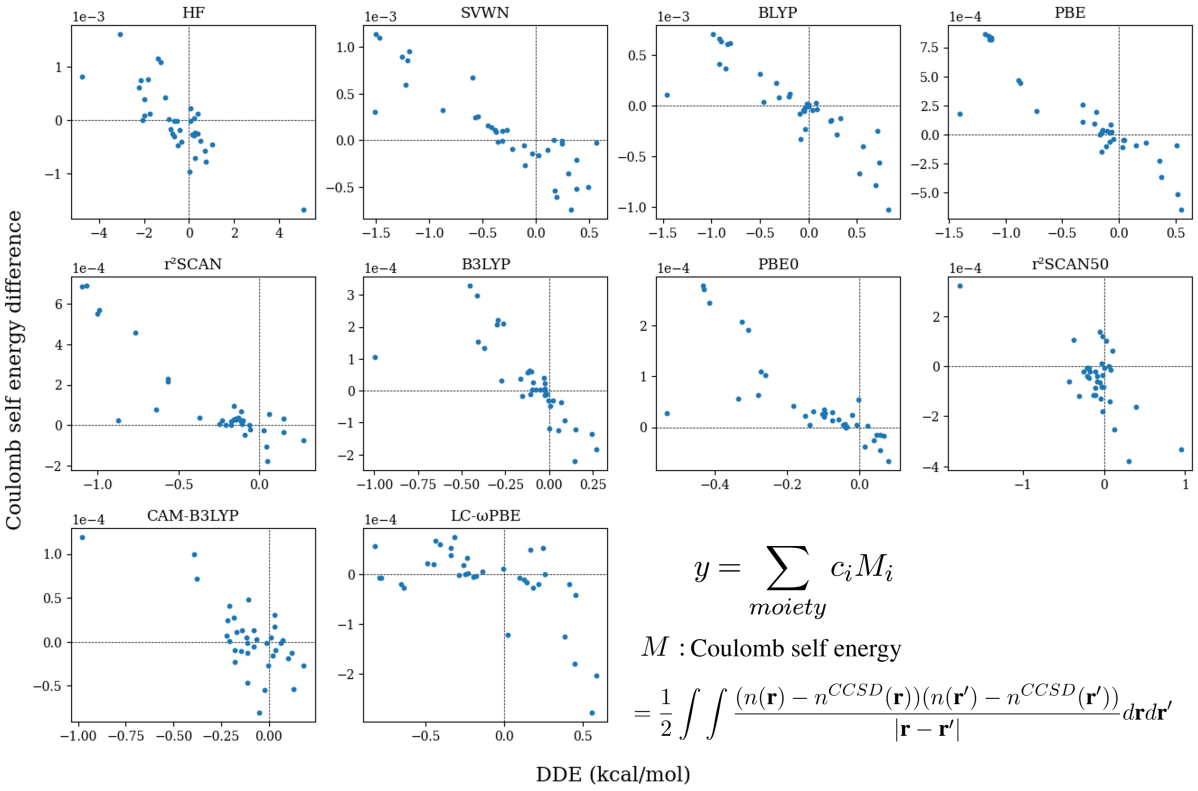

Figure S13: Relation between density-driven error (DDE) and Coulomb self-energy differences for the 36 selected reactions (listed in Table S9), evaluated across various density functionals. CCSD densities are used as the reference. The equation used to calculate the density metric is provided at the bottom right corner of the figure.

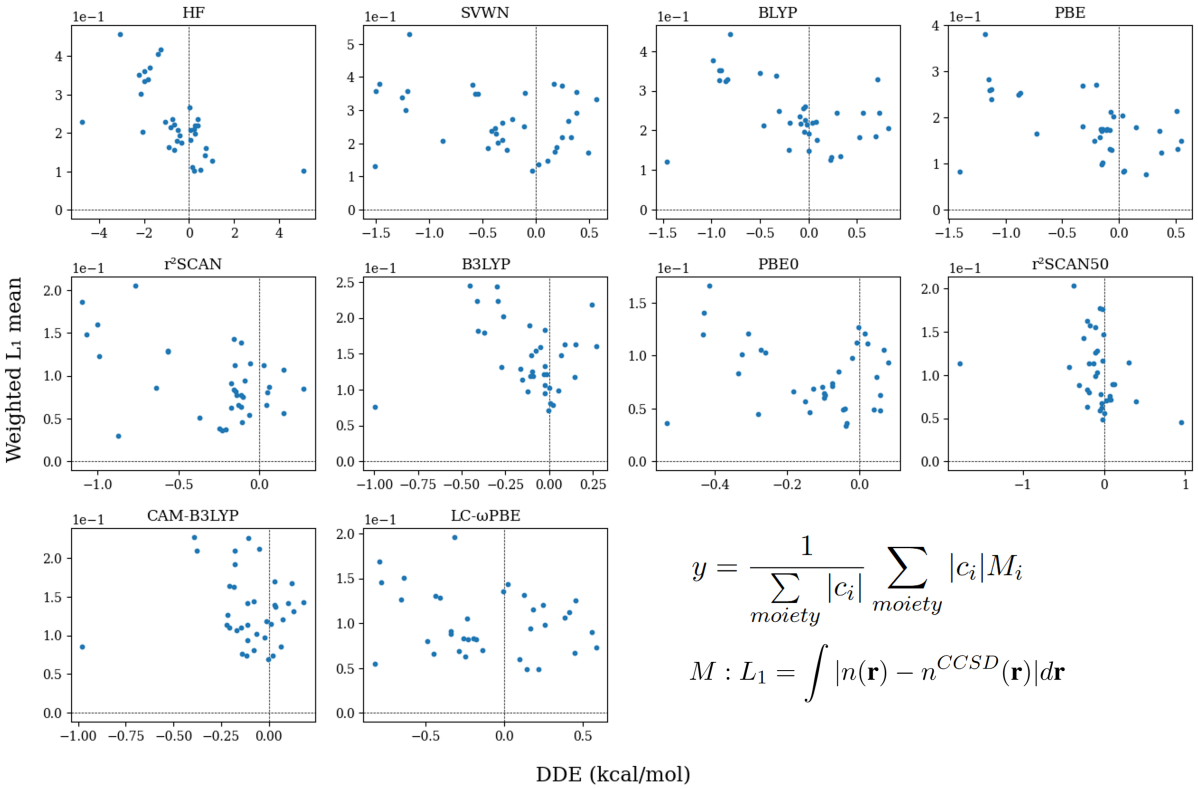

Figure S14: Relation between density-driven error (DDE) and L_1 norm differences for the 36 selected reactions (listed in Table S9), evaluated across various density functionals. CCSD densities are used as the reference. The equation used to calculate the density metric is provided at the bottom right corner of the figure.

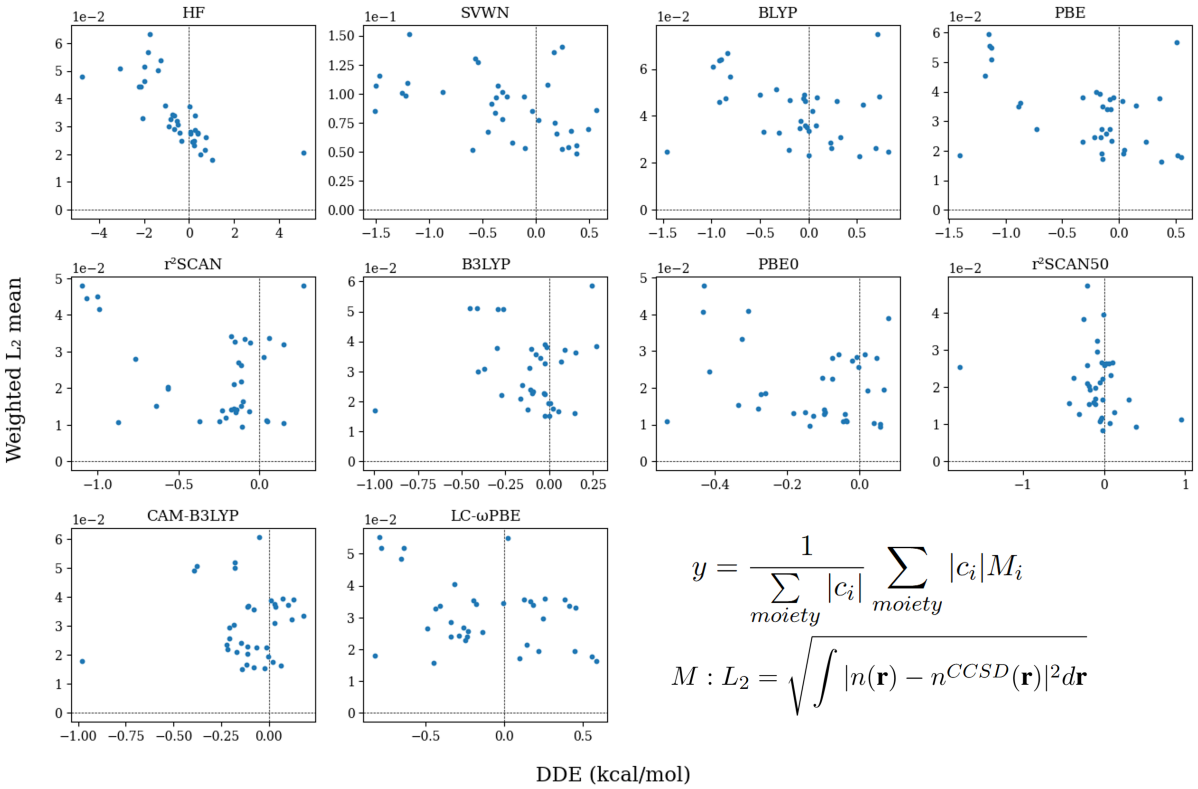

Figure S15: Relation between density-driven error (DDE) and L_2 norm differences for the 36 selected reactions (listed in Table S9), evaluated across various density functionals. CCSD densities are used as the reference. The equation used to calculate the density metric is provided at the bottom right corner of the figure.

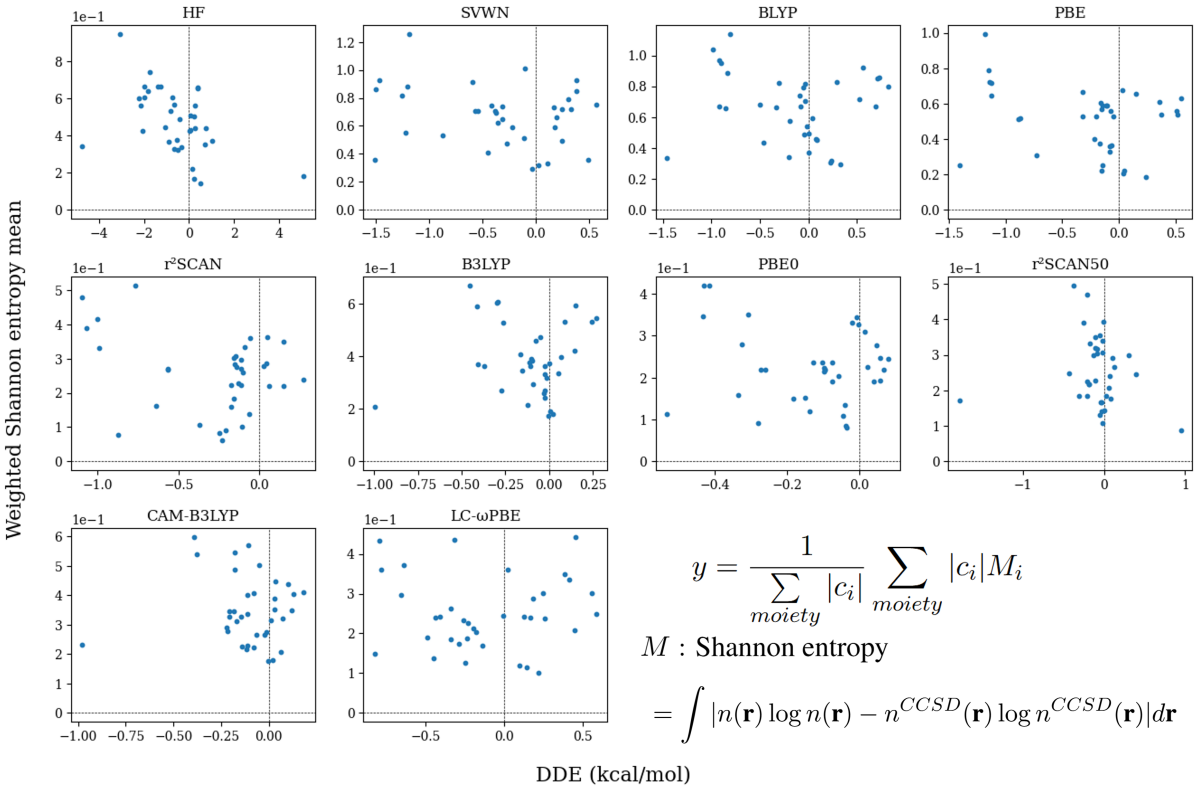

Figure S16: Relation between density-driven error (DDE) and Shannon entropy [12] differences for the 36 selected reactions (listed in Table S9), evaluated across various density functionals. CCSD densities are used as the reference. The equation used to calculate the density metric is provided at the bottom right corner of the figure.

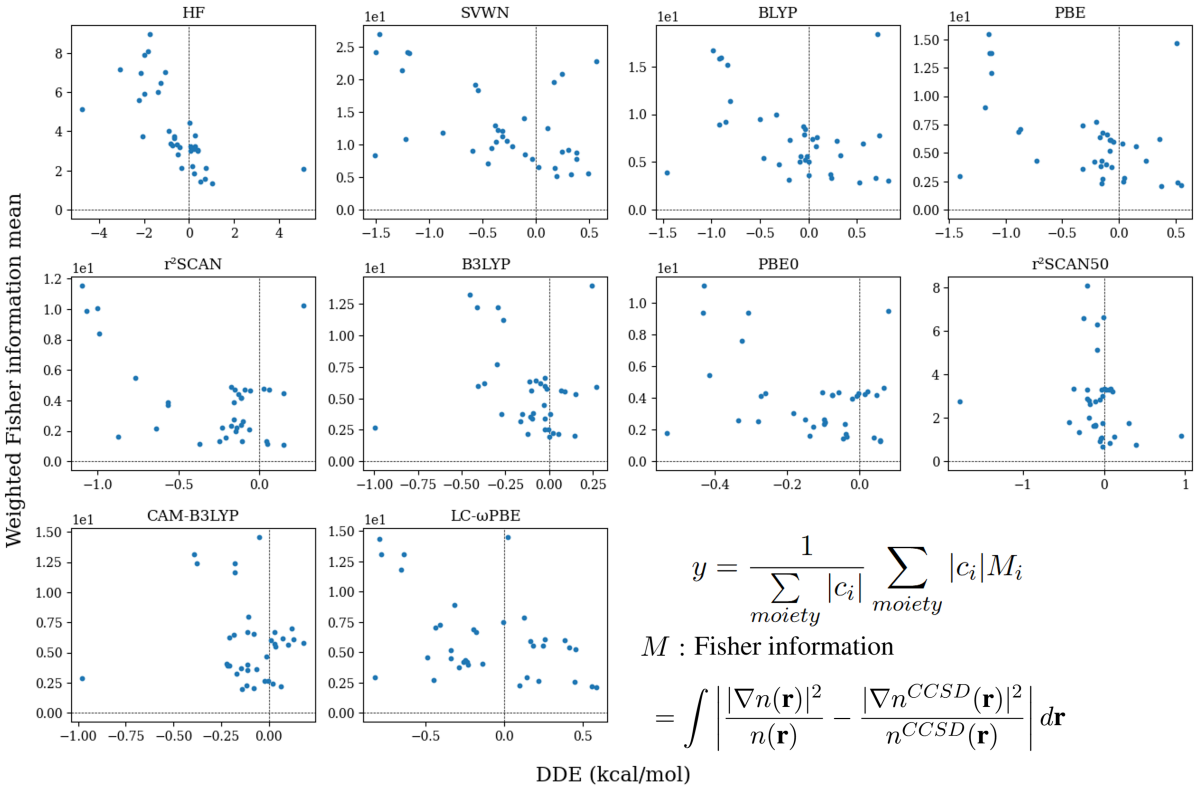

Figure S17: Relation between density-driven error (DDE) and Fisher information [13] differences for the 36 selected reactions (listed in Table S9), evaluated across various density functionals. CCSD densities are used as the reference. The equation used to calculate the density metric is provided at the bottom right corner of the figure.

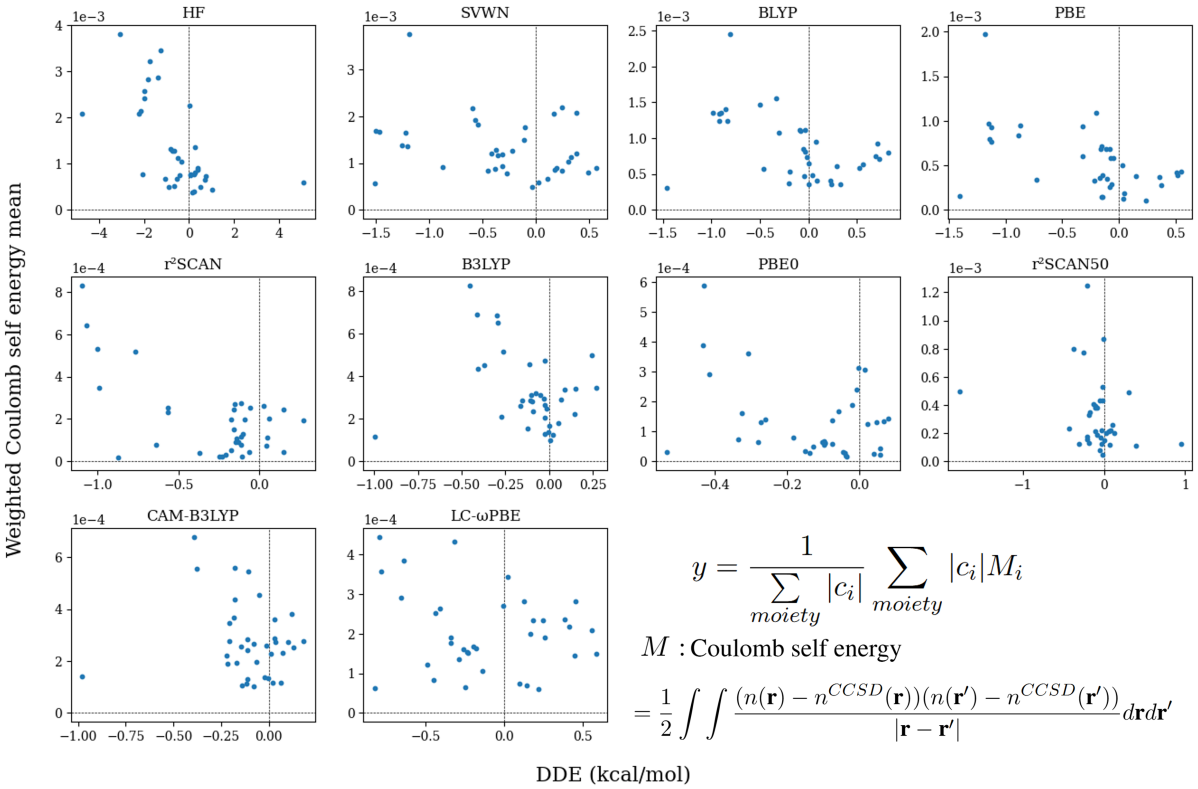

Figure S18: Relation between density-driven error (DDE) and Coulomb self-energy differences for the 36 selected reactions (listed in Table S9), evaluated across various density functionals. CCSD densities are used as the reference. The equation used to calculate the density metric is provided at the bottom right corner of the figure.

REFERENCES

[1] Lars Goerigk, Andreas Hansen, Christoph Bauer, Stephan Ehrlich, Asim Najibi, and Stefan Grimme. A look at the density functional theory zoo with the advanced gmtkn55 database for general main group thermochemistry, kinetics and noncovalent interactions. *Phys. Chem. Chem. Phys.*, 19(48):32184–32215, 2017.

[2] Thom H Dunning Jr. Gaussian basis sets for use in correlated molecular calculations. i. the atoms boron through neon and hydrogen. *J. Chem. Phys.*, 90(2):1007–1023, 1989.

[3] Aaron D Kaplan, Chandra Shahi, Pradeep Bhetwal, Raj K Sah, and John P Perdew. Understanding density-driven errors for reaction barrier heights. *J. Chem. Theory Comput.*, 19(2):532–543, 2023.

[4] Qiming Sun, Timothy C Berkelbach, Nick S Blunt, George H Booth, Sheng Guo, Zhendong Li, Junzi Liu, James D McClain, Elvira R Sayfutyarova, Sandeep Sharma, et al. Pyscf: the python-based simulations of chemistry framework. *Wiley Interdiscip. Rev. Comput. Mol. Sci.*, 8(1):e1340, 2018.

[5] Qiming Sun, Xing Zhang, Samragni Banerjee, Peng Bao, Marc Barbry, Nick S Blunt, Nikolay A Bogdanov, George H Booth, Jia Chen, Zhi-Hao Cui, et al. Recent developments in the pyscf program package. *J. Chem. Phys.*, 153(2), 2020.

[6] Gustavo E Scuseria. Analytic evaluation of energy gradients for the singles and doubles coupled cluster method including perturbative triple excitations: Theory and applications to foof and cr2. *J. Chem. Phys.*, 94(1):442–447, 1991.

[7] John D Watts, Jürgen Gauss, and Rodney J Bartlett. Coupled-cluster methods with noniterative triple excitations for restricted open-shell hartree–fock and other general single determinant reference functions. energies and analytical gradients. *J. Chem. Phys.*, 98(11):8718–8733, 1993.

[8] Rodney J Bartlett and Monika Musiał. Coupled-cluster theory in quantum chemistry. *Rev. Mod. Phys.*, 79(1):291–352, 2007.

[9] Antonio Bauza, Ibon Alkorta, Antonio Frontera, and Jose Elguero. On the reliability of pure and hybrid dft methods for the evaluation of halogen, chalcogen, and pnicogen bonds involving anionic and neutral electron donors. *J. Chem. Theory Comput.*, 9(11):5201–5210, 2013.

[10] A Otero-De-La-Roza, Erin R Johnson, and Gino A DiLabio. Halogen bonding from dispersion-corrected density-functional theory: The role of delocalization error. *J. Chem. Theory Comput.*, 10(12):5436–5447, 2014.

[11] George D Purvis III and Rodney J Bartlett. A full coupled-cluster singles and doubles model: The inclusion of disconnected triples. *J. Chem. Phys.*, 76(4):1910–1918, 1982.

[12] C. E. Shannon. A mathematical theory of communication. *Bell Syst. Tech. J.*, 27(3):379–423, 1948.

[13] R. A. Fisher. Theory of statistical estimation. *Math. Proc. Camb. Philos. Soc.*, 22(5):700–725, 1925.